Slope Control in Western Boundary Currents

SANG-KI LEE

Department of Oceanography, Inha University, Incheon, Korea

J. L. PELEGRÍ

Facultad de Ciencias del Mar, Universidad de Las Palmas de Gran Canaria, Las Palmas de Gran Canaria, Spain

JOHN KROLL

Department of Mathematics and Statistics, Old Dominion University, Norfolk, Virginia

(Manuscript received 4 August 2000, in final form 7 May 2001)

ABSTRACT

An analytic solution is presented for the steady-state depth-averaged western boundary current flowing over the continental slope by combining three highly idealized models: the Stommel model, the Munk model, and the arrested topographic wave model. The main vorticity balance over the slope is between planetary vorticity advection and the slope-induced bottom stress torque, which is proportional to $rv(h^{-1})_x$ where r is the Rayleigh friction coefficient, h is the water depth, and v is the meridional velocity. This slope-induced torque provides the necessary source of vorticity for poleward flow over the slope, its simple interpretation being that vorticity is produced because the bottom stress has to act over the seaward-deepening water column. The character of the solution depends on the slope α as well as on the assumed bottom drag coefficient, and the length scale of the boundary current is $\sim\sqrt{2r/(\beta\alpha)}$. It is further shown that, if the depth-averaged velocity flows along isobaths, then the stretching of water columns associated with cross-isobath geostrophic flow, which compensates bottom Ekman transport, is identical to the slope-induced torque by the geostrophic velocities.

1. Introduction

The classical theories underlying our understanding of large-scale ocean circulation are mainly based on beta-plane and flat-bottom assumptions (e.g., Stommel 1948; Munk 1950). There is little observational evidence on the influence of topographic features on midocean mean circulation, probably because of the surface-trapped nature of wind-driven circulation in a stratified ocean. This has likely dwarfed the importance of topography in process-oriented models of the subtropical gyres, in particular the role played by topographic features in lateral boundaries (e.g., Huang 1991). The importance of the slope at the ocean boundaries became clear in Warren's (1963) idealized model on the meandering of a western boundary current due to vortex stretching over a sloping bottom. Holland (1973) did a numerical study to find that the continental slope has a profound influence on the western boundary current and the midcirculation gyre. Salmon (1992) investigated the similarity solutions for the Stommel-type western boundary current over a sloping bottom. His steady-state solution indicates a southwestern intensification due to both the planetary and the topographic beta effects. More recently Griffiths and Veronis (1997, 1998) reported a similar result from laboratory and theoretical studies.

Coastal oceanographers, on the contrary, have normally focused on *f*-plane dynamics, treating bottom topography as a principal constraint to the character of the flow (e.g., Csanady 1982, 1988). Tidal and wind-induced currents within the continental shelf are greatly controlled by the shelf topography. Topographic or coastal-trapped waves are another clear example, within the continental shelf and slope, resulting from vortex stretching induced by cross-isobath velocities.

The connection between these two rather opposite approaches has come slowly. Csanady (1988), in a massive and intense paper, summarized progress made on the role of the continental slope in ocean circulation. He illustrated a number of examples of what he called the fundamental slope effect on ocean circulation: velocities perpendicular to depth contours are responsible for the stretching or squashing of vortex tubes, in what may be interpreted as torque induced by bottom pres-

Corresponding author address: Dr. Sang-Ki Lee, Maritime Research Institute, Samsung Heavy Industries, Koje, Kyungnam 656-710, Korea.
E-mail: sklee621@hanmail.net

sure. Csanady (1979, 1988) pointed at the possibility that bottom pressure torque, induced by an alongshore pressure gradient found on the east coast of North America, may balance planetary vorticity advection. A related issue is the potential contribution of baroclinicity to bottom pressure torque, what has been named the joint effect of baroclinicity and relief (Sarkisyan and Ivanov 1971; Simons 1979; Shaw and Csanady 1983; Huthnance 1984; Csanady 1988).

A particular example of the fundamental slope effect is the arrested topographic wave, where bottom pressure torque is balanced by wind and bottom stress torque (Csanady 1978, 1982, 1988). This balance has been used to model the shelf circulation problems. Csanady (1988), for example, illustrated a situation where coupling between the coastal and deep oceans takes place in a shelf-edge boundary layer stretching 55 km on the shelf side and 17 km on the slope side, in which the bottom stress torque is as large as bottom pressure torque. These calculations, applied to western boundary currents in contact with the sea bottom, suggested that bottom friction is indeed important but only in the upper slope waters, probably down to depths of about 300 m.

A key factor in the above discussion is the parameterization of bottom friction. Csanady (1976) justified that a linear friction law, with a constant Rayleigh friction coefficient, is adequate when considering the momentum equations for the mean flow. This result is coherent with the linear decay term that appears in the vorticity equation, with bottom friction parameterized using a constant eddy viscosity model. A linear friction law with a constant coefficient is, however, a gross simplification on how bottom stress is transferred from the bottom boundary layer into the interior ocean, in particular on how it reduces the strength of vortex tubes.

Recently a lot of interest has arisen on the potential role of the bottom boundary layer in transferring properties to the deep ocean (for a review see Garret et al. 1993), making clear the necessity of a proper representation of this layer. Several observational works (Thorpe 1987; Thorpe et al. 1990; Lentz and Trowbridge 1991) have shown that the bottom boundary layer at continental slopes has large spatial and temporal variability depending, among other things, on current magnitude and direction. These works have been followed by theoretical studies of issues such as the blockage of Ekman transport in the bottom boundary layer, the interaction between the interior flow and the boundary layer, and the transfer of mass and vorticity into the interior ocean along isopycnals (e.g., Thorpe 1987; Garret 1990; McCready and Rhines 1991, 1993; Garret et al. 1993; Trowbridge and Lentz 1991; Csanady and Pelegrí 1995; Chapman and Lentz 1997). A corollary from these works has been the recognition of the difficulties in specifying the bottom boundary layer dynamics and, hence, in finding a proper specification of the bottom boundary conditions for the interior vorticity.

In this study we look for a steady-state solution of the depth-averaged western boundary current over a continental slope, with the bottom friction representation commonly used for coastal ocean studies. The bottom stress (a force per unit area) divided by the water depth gives a force per unit volume and its curl is proportional to the bottom stress torque acting over the whole water column, which modifies the strength of the interior vortex tubes. The bottom stress torque is interpreted as resulting from the contribution of two terms. The first one is proportional to the bottom stress curl, with bottom stress directly proportional but opposite to the velocity, acting over an ocean of constant depth. This contribution produces bottom Ekman transport analogous to that usually found with the quasigeostrophic approximation, and commonly interpreted as causing stretching/shrinking of interior vortex tubes. The second contribution, called the slope-induced bottom stress torque, is related to the different response experienced by water columns of different thickness when exposed to the same bottom stress. It is nonzero, even with null interior vorticity, and suggests an additional mechanism of coupling between the interior flow and the boundary layer. We also investigate the behavior of the quasigeostrophic vorticity equation over the sloping bottom. For the case of depth-averaged flow along isobaths we find that the geostrophic vorticity may change because of stretching/squashing of the interior water columns due to cross-isobath geostrophic flow. This term resembles the slope-induced bottom torque, but with the torque now induced by the geostrophic rather than the depth-averaged flow.

We are really not interested in how accurate this representation may be, particularly since we recognize the limitation involved in neglecting the important role of stratification. But, we have been indeed attracted by the fact that such a simple modification introduces new and realistic elements to the classical homogeneous solution. Furthermore, for the special case of a linear depth profile, the equation has an exact analytical solution. Our hope is that it may motivate further research on the behavior and importance of the bottom boundary layer in the vorticity balance within western boundary currents.

2. The vorticity equation over the slope

a. Ekman pumping on a sloping bottom

The backbone for our understanding of large-scale ocean circulation is Ekman pumping at the boundaries, which drives the geostrophic flow in the interior ocean. In the quasigeostrophic approximation the usual manner to obtain the vorticity equation describing this balance is to scale the momentum equations and to express the dependent variables as asymptotic series in terms of a small parameter, the Rossby number. The lowest order fields are geostrophic and the quasigeostrophic vorticity equation is obtained as the curl of the next order equa-

tions. Using the continuity equation it becomes (Pedlosky 1979)

$$\frac{D\zeta_g}{Dt} + \beta v_g = A_h \nabla^2 \zeta_g + \frac{f}{h}(w_t - w_b). \tag{1}$$

The nomenclature is the usual: u_g and v_g are the cross-slope (eastward, along x) and alongslope (northward, along y) geostrophic velocities, $D/Dt \equiv \partial/\partial t + \mathbf{u}_g \cdot \nabla$ is the material derivative calculated using the geostrophic velocities, $\zeta_g = \partial v_g/\partial x - \partial u_g/\partial y$ is the geostrophic relative vorticity, h is the water depth, $f = f_o + \beta y$ is the planetary vorticity in the beta-plane approximation, A_h is the lateral eddy viscosity, and w_t and w_b represent the vertical velocities at the top and bottom boundaries, respectively.

Even at the continental slope the bottom has a rather gentle slope; for example, where the Gulf Stream flows over the continental slope typical values are 2000 m in 50 km giving 2×10^{-2}. Pedlosky (1979) has shown that in this case lateral friction is negligible and the vertical velocity at the bottom is given by

$$w_b = -\mathbf{u}_g \cdot \nabla h + \left(\frac{A_v}{2f_o}\right)^{1/2} \zeta_g, \tag{2}$$

where A_v is the vertical eddy viscosity. In the quasigeostrophic theory this vertical velocity is considered as resulting from both cross-isobath bottom flow and nonconstant Ekman transport within the bottom boundary layer, and has been interpreted as causing stretching/squashing of the interior vortex tubes. A point to note here is that this expression for w_b is obtained under the condition of constant A_v.

Salmon (1992) studied a similar vorticity balance on a sloping bottom. In his vorticity equation, however, the depth h in the denominator of the Ekman pumping term [Eq. (1)] is replaced by the deep water depth H. This assumption greatly simplifies the calculation procedure but, as we will see below, it obscures some aspects of the boundary layer physics. Griffiths and Veronis (1998) used an analogous method to obtain a series solution for Eq. (2) in powers of $E^{1/2}$, where E is the Ekman number.

b. The depth-averaged vorticity equation

One alternative method to derive the vorticity equation, commonly used in coastal ocean literature, is to integrate the momentum equations from the sea surface to the bottom and then take the curl of these vertically integrated equations (e.g., Csanady 1982). The depth-averaged momentum equations are

$$\frac{Du}{Dt} - fv = -g\frac{\partial \eta}{\partial x} - \frac{\tau_{bx}}{\rho h}, \tag{3a}$$

$$\frac{Dv}{Dt} + fu = -g\frac{\partial \eta}{\partial y} - \frac{\tau_{by}}{\rho h}, \tag{3b}$$

where u and v are the cross-slope (eastward, along x) and alongslope (northward, along y) depth-averaged velocities, η is the surface water elevation, ρ is the density, and g is the gravity acceleration. The bottom friction forces are taken to depend linearly on the depth-averaged velocity as $\tau_{bx} = r\rho u$, $\tau_{by} = r\rho v$, where r is the Rayleigh friction coefficient with units of meters per second. After cross-differentiation these equations lead to

$$\frac{D\zeta}{Dt} + \beta v = A_h \nabla^2 \zeta + \frac{f}{h}(\varpi_t - \varpi_b). \tag{4}$$

The nomenclature is as before, but now the material derivative $D/Dt \equiv \partial/\partial t + \mathbf{u} \cdot \nabla$ and the relative vorticity $\zeta = \partial v/\partial x - \partial u/\partial y$ are calculated using the depth-averaged velocities, and ϖ_t and ϖ_b are variables analogous to the vertical velocities at the top and bottom boundaries, respectively. The expression for this bottom vertical velocity is as follows:

$$\begin{aligned} \varpi_b &= -\mathbf{u} \cdot \nabla h + \frac{h}{\rho f}\left[\frac{\partial}{\partial x}\left(\frac{\tau_{by}}{h}\right) - \frac{\partial}{\partial y}\left(\frac{\tau_{bx}}{h}\right)\right] \\ &= \underbrace{-\mathbf{u} \cdot \nabla h}_{\text{(i)}} + \underbrace{\frac{r}{f}\zeta}_{\text{(ii)}} - \underbrace{\frac{r}{fh}\left(v\frac{\partial h}{\partial x} - u\frac{\partial h}{\partial y}\right)}_{\text{(iii)}}. \end{aligned} \tag{5}$$

The last equality assumes constant r. The first contribution to this bottom vertical velocity comes from the cross-isobath depth-averaged flow. The other contributions come from the bottom stress torque, their physical interpretation arising if we consider the following decomposition:

$$\begin{aligned} &h\frac{\partial}{\partial x}\left(\frac{\tau_{by}}{h}\right) - h\frac{\partial}{\partial y}\left(\frac{\tau_{bx}}{h}\right) \\ &\quad = \left[\left(\frac{\partial \tau_{by}}{\partial x} - \frac{\partial \tau_{bx}}{\partial y}\right) + \left(\frac{\tau_{bx}}{h}\frac{\partial h}{\partial y} - \frac{\tau_{by}}{h}\frac{\partial h}{\partial x}\right)\right]. \end{aligned} \tag{6}$$

The bottom stress torque may now be considered as the result of the two terms in the right-hand side of (6). The first term is the bottom stress curl already discussed by other authors in coastal literature (e.g., Csanady 1988). It is proportional to the torque acting over the squared bottom face of a column of constant depth h. This may be readily calculated expanding τ_{bx} and τ_{by} as Taylor series and integrating the torque $(\tau_{by}x - \tau_{bx}y)$ over the squared bottom face. The second term is due to the volume force imparted by the bottom stress $(\tau_{bx}/h, \tau_{by}/h)$, which retards different amounts of water mass depending on the actual water depth, that is, on the slope $\partial h/\partial y$, $\partial h/\partial x$. We name this second term as the slope-induced or slope contribution to the bottom stress torque.

Equation (5) has three terms, and the first two terms are fully analogous to those in the bottom vertical velocity of the quasigeostrophic equation (2). These terms

are (i) the cross-isobath flow term and (ii) the term depending on the vorticity, although it is important to emphasize that here we are dealing with depth-averaged velocities. If the geostrophic and depth-averaged velocities were equal, then these two vorticity terms in both equations would be identical provided that $r = (A_v f_o/2)^{1/2}$. In the depth-averaged vorticity equation, the vorticity-dependent term (ii) is the result of bottom stress curl (or bottom stress torque for constant water depth), while in quasigeostrophic theory it is identified as resulting from the expansion/compression of interior vortex tubes. Recent results have shown that within the boundary layer A_v is rather large (e.g., Garret et al. 1993). Using typical values $A_v = 10^{-4} \sim 10^{-2}$ m^2 s^{-1} and $f = 10^{-4}$ s^{-1} we obtain $r = 10^{-4} \sim 10^{-3}$ m s^{-1}, which is of the order of magnitude usually quoted for the Rayleigh friction coefficient (e.g., Weatherly 1972; Csanady 1976, 1982). This number may also be compared with estimates for r/H of 100 days^{-1}, which gives $r \sim 10^{-4}$ m s^{-1} (e.g., Gill 1982). This indeed suggests that these two terms are analogous, although with the depth-averaged velocities in Eq. (5) and the geostrophic velocities in Eq. (2). Note that the analogy would have disappeared if we had used a constant depth in the last term of Eq. (1), as assumed by Salmon (1992) and Griffiths and Veronis (1998).

Equation (5) has one additional term, the slope-induced bottom stress torque (iii) that depends on the velocity, the water depth, and the bottom slope. To illustrate the role played by the slope-induced bottom torque let us consider a western boundary current flowing northward along a continental slope (Northern Hemisphere). In the absence of a slope the sign of the bottom torque will depend only on the curl of the bottom stress. In particular, if the boundary current initially has zero relative vorticity and the bottom boundary layer is spatially uniform (constant r or A_v), then the torque is zero. However, if the water depth increases offshore, the bottom stress has to act over increasingly thicker water columns and produces a bottom torque, resulting in a gain of positive vorticity by the northward flow, even if the curl of the bottom stress is negative. A simple scheme that portrays the slope-induced bottom torque is illustrated in Fig. 1. Note that the size and sign of the slope-induced torque depends on the bottom slope: within a western boundary current flowing over a steep continental slope it opposes the bottom stress curl term in the cyclonic side of the stream.

This derivation of the depth-averaged vorticity equation illustrates that there are three different mechanisms for modifying the interior vorticity:

1) cross-isobath flow of the depth-averaged velocity;
2) bottom stress curl, or bottom stress torque for constant water depth; and
3) slope-induced bottom stress torque that results from the coupling between the depth-averaged current, the bottom slope, and the dynamics of the bottom boundary layer (here simply specified as a constant bottom drag coefficient).

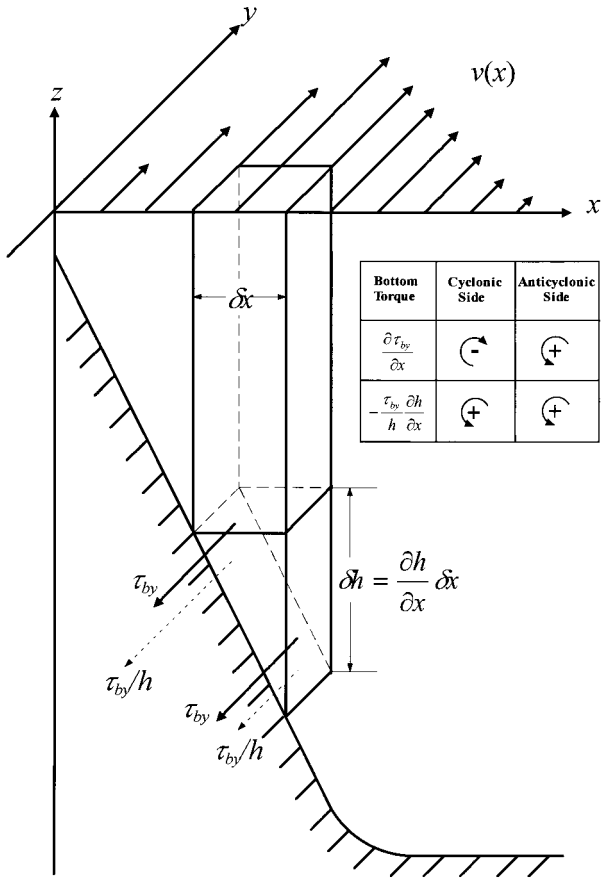

FIG. 1. Sketch of the slope contribution to the bottom stress torque. The boundary jet gains positive (negative) vorticity for northward (southward) flow.

c. Cross-isobath flow

Let us further investigate the analogy between Eqs. (2) and (5). With this purpose we write the depth-averaged velocities as

$$u = \frac{u_g h + u_E \delta_E}{h} \tag{7a}$$

$$v = \frac{v_g h + v_E \delta_E}{h}, \tag{7b}$$

where δ_E stands for the thickness of the bottom Ekman layer and u_E and v_E indicate the x and y components of the Ekman velocity. The use of Eq. (7) leads to

$$u\frac{\partial h}{\partial x} + v\frac{\partial h}{\partial y} = \left(u_g\frac{\partial h}{\partial x} + v_g\frac{\partial h}{\partial y}\right) + \left(\frac{u_E\delta_E}{h}\frac{\partial h}{\partial x} + \frac{v_E\delta_E}{h}\frac{\partial h}{\partial y}\right). \tag{8}$$

The components of the bottom Ekman transport, $u_E\delta_E$ and $v_E\delta_E$, are related to the bottom stress as follows:

$$u_E\delta_E = -\frac{r}{f}v_g, \tag{9a}$$

$$v_E\delta_E = \frac{r}{f}u_g. \tag{9b}$$

Substitution of these expressions in Eq. (8) leads to

$$u_g\frac{\partial h}{\partial x} + v_g\frac{\partial h}{\partial y} = \left(u\frac{\partial h}{\partial x} + v\frac{\partial h}{\partial y}\right) + \frac{r}{fh}\left(v_g\frac{\partial h}{\partial x} - u_g\frac{\partial h}{\partial y}\right). \tag{10}$$

This shows that, if the depth-averaged flow is along isobaths, then the stretching due to cross-isobath geostrophic flow is analogous to a slope-induced bottom torque by the geostrophic flow. For this case the bottom vertical velocity in the quasigeostrophic vorticity equation and its counterpart in the depth-averaged vorticity equation have exactly the same dependence:

$$w_b = -\left(u_g\frac{\partial h}{\partial x} + v_g\frac{\partial h}{\partial y}\right) + \frac{r}{f}\zeta_g = -\frac{r}{fh}\left(v_g\frac{\partial h}{\partial x} - u_g\frac{\partial h}{\partial y}\right) + \frac{r}{f}\zeta_g, \tag{11a}$$

$$\varpi_b = -\left(u\frac{\partial h}{\partial x} + v\frac{\partial h}{\partial y}\right) + \frac{r}{f}\zeta - \frac{r}{fh}\left(v\frac{\partial h}{\partial x} - u\frac{\partial h}{\partial y}\right) = \frac{r}{f}\zeta - \frac{r}{fh}\left(v\frac{\partial h}{\partial x} - u\frac{\partial h}{\partial y}\right). \tag{11b}$$

In the depth-averaged vorticity equation the cross-isobath term is zero while in the quasigeostrophic vorticity equation the stretching related to the cross-isobath geostrophic flow has exactly the same dependence as the slope-induced torque.

If there is a coast, then the flow normal to the coast has to be zero, what is usually called the coastal constraint. This condition will hold far from the coast only when there are no changes in the alongshore direction; that is, for poleward flow, onshore bottom Ekman transport will be compensated through offshore geostrophic transport such that the total cross-isobath flow is zero. We have just shown, however, that, when the depth-averaged flow is along isobaths, a compensating geostrophic flow always exists, regardless of the presence of the coast, and the slope-induced bottom torque is exactly equal to the cross-isobath stretching term.

3. Model formulation

Equation (1) with (2) has been referred to as the quasigeostrophic vorticity equation, and Eq. (4) with (5) as the depth-averaged vorticity equation. For the particular case of depth-averaged along-isobath flow we have shown that the mathematical dependence is exactly the same, with the forcing terms given by Eq. (11). In this and the following two sections we will examine the solution of Eq. (1) or (4), forced by (11). The analysis of the differences between the geostrophic and the depth-averaged solutions will be left for the discussion and conclusions.

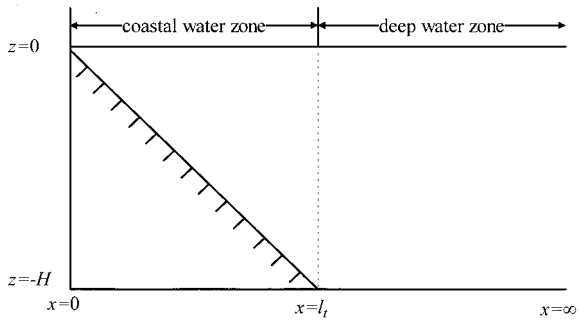

FIG. 2. Sketch of the model configuration. The model domain is divided into the coastal zone of linear bottom slope and the deep water zone of constant depth H.

If the depth-averaged flow is steady and parallel to the coastline and the vorticity input by the local wind stress is not important, Eq. (1) or (4), with (11), is

$$\beta v = A_h\frac{d^3v}{dx^3} - \frac{r}{h}\frac{dv}{dx} + \frac{rv}{h^2}\frac{dh}{dx}. \tag{12}$$

The model variables are made nondimensional by scaling the horizontal coordinates by the Munk length $l_m[=(A_h/\beta)^{1/3}]$, the vertical by the deep ocean depth H, and the horizontal velocities by $\psi_o/H/l_m$ where ψ_o is the volume transport stream function at $x = \infty$. The model ocean includes the coastal area of uniform slope H/l_t and the deep ocean of constant depth, that is,

$$h(x) = \begin{cases} H/l_t x, & 0 < x < l_t/l_m \\ 1, & l_t/l_m < x, \end{cases} \tag{13}$$

as illustrated schematically in Fig. 2, where l_t is the length of the sloping zone. Then the dimensionless form of Eq. (12) is

$$v''' - \frac{\alpha_1}{x}v' + \left(\frac{\alpha_1}{x^2} - 1\right)v = 0 \quad \text{for } x < l_t/l_m, \tag{14}$$

$$v''' - \alpha_2 v' - v = 0 \quad \text{for } x > l_t/l_m, \tag{15}$$

where $l_s(=r/\beta H)$ is the Stommel length and the coefficients α_1 and α_2 are expressed in terms of the three different length scales; that is,

$$\alpha_1 = \frac{l_s l_t}{l_m^2}, \tag{16a}$$

$$\alpha_2 = \frac{l_s}{l_m}. \tag{16b}$$

The governing equations (14) and (15) are two third-order ordinary differential equations; therefore six boundary conditions are required to solve them. At $x = 0$ a no-slip condition is applied and at $x = \infty$ the solution must be bounded. Other boundary conditions are that velocity, shear stress, and pressure must be continuous across the interface (White 1991). Accordingly, the matching conditions at $x = l_t$ (in dimensional form) are

$$v_c = v_d, \tag{17a}$$

$$A_h \frac{dv_c}{dx} = A_h \frac{dv_d}{dx}, \tag{17b}$$

$$\eta_c = \eta_d, \tag{17c}$$

where the subscripts c and d represent the coastal side and deep-ocean sides, respectively. In order to express the pressure continuity condition (17c) in terms of the velocity variables, we need to look at the momentum equations from which the vorticity equations are derived. They are, in dimensional form,

$$-(f_o + \beta y)v = -g\frac{\partial \eta}{\partial x}, \tag{18}$$

$$0 = -g\frac{\partial \eta}{\partial y} + A_h \frac{\partial^2 v}{\partial x^2} - \frac{r}{h}v. \tag{19}$$

Close inspection of these equations reveals that, since the velocity is only a function of x, the general form of the surface elevation is

$$\eta(x) = \eta_o(x) + \eta_1(x)y. \tag{20}$$

Therefore, the y momentum equation (19) becomes

$$0 = -g\eta_1 + A_h \frac{\partial^2 v}{\partial x^2} - \frac{r}{h}v. \tag{21}$$

Due to the continuity conditions of pressure (17c) and velocity (17a), Eq. (21) becomes

$$A_h \frac{d^2 v_c}{dx^2} = A_h \frac{d^2 v_d}{dx^2} \quad \text{at } x = l_t. \tag{22}$$

The continuity of the y-independent surface elevation $\eta_o(x)$ is automatically satisfied since the velocity is continuous and finite at the interface. Finally, the following (dimensional) condition determines the amplitude of the solution:

$$\int_0^{l_t} v_c h\, dx + \int_{l_t}^{\infty} v_d h\, dx = \psi_o. \tag{23}$$

The result is that we have six boundary conditions; hence, they are sufficient to solve the vorticity equations (14) and (15). For future convenience, the six boundary conditions are summarized here in nondimensional form:

$$v_c(0) = 0, \tag{24a}$$

$$v_d(\infty) \text{ is bounded} \tag{24b}$$

$$v_c\left(\frac{l_t}{l_m}\right) = v_d\left(\frac{l_t}{l_m}\right), \tag{24c}$$

$$v_c'\left(\frac{l_t}{l_m}\right) = v_d'\left(\frac{l_t}{l_m}\right), \tag{24d}$$

$$v_c''\left(\frac{l_t}{l_m}\right) = v_d''\left(\frac{l_t}{l_m}\right), \tag{24e}$$

$$\frac{l_m}{l_t}\int_0^{l_t/l_m} v_c x\, dx + \int_{l_t/l_m}^{\infty} v_d dx = 1. \tag{24f}$$

4. The analytic solution

An analytic solution in terms of infinite series can readily be found for the third-order system (14) and (15) with the boundary, continuity, and flow conditions (24a)–(24f). Considering Eq. (14) first, we can show that there exists two linearly independent series solutions of the form

$$v_1(x) = \sum_{n=0}^{\infty} a_n x^n, \tag{25a}$$

$$v_2(x) = \sum_{n=0}^{\infty} b_n x^n, \tag{25b}$$

where the coefficients are given recursively by

$$a_n = \frac{a_1(n-2)a_{n-1} + a_{n-3}}{n(n-1)(n-2)}, \qquad a_{0,2} = 0, \quad a_1 = 1, \tag{26a}$$

$$b_n = \frac{a_1(n-2)b_{n-1} + b_{n-3}}{n(n-1)(n-2)}, \qquad b_{0,1} = 0, \quad b_2 = 1. \tag{26b}$$

The third independent solution, $v_3(x)$, can be found knowing the previous two and using the reduction

$$v_3 = v_2 \int \frac{v_1}{W^2}\, dx - v_1 \int \frac{v_2}{W^2}\, dx, \tag{27}$$

where $W = v_1 v_2' - v_2 v_1'$ is the Wronskian. Thus the general solution of (14) is

$$v = C_1 v_1 + C_2 v_2 + C_3 v_3. \tag{28}$$

However, we can show that $v_3(0) = 1/2$ and, since $v_1(0) = v_2(0) = 0$, the boundary condition at $x = 0$ is satisfied only if $C_3 = 0$. Therefore, the rather complicated solution v_3 is not part of our solution.

The characteristic polynomial for the constant coefficient equation (15) is $m^3 - \alpha_2 m - 1 = 0$. For $\alpha_2 \geq$

0, there is one root whose real part is always positive and therefore eliminated by the condition at x going to infinity. The two needed roots whose real parts are always negative are

$$m_{1,2} = -\frac{A+B}{2} \pm \frac{\sqrt{3}}{2}(A-B)i, \qquad \alpha_2 < \frac{3}{\sqrt[3]{4}}, \quad (29a)$$

where

$$\begin{pmatrix} A \\ B \end{pmatrix} = \frac{1}{\sqrt[3]{2}}\left(1 \pm \sqrt{1 - \frac{4\alpha_2^3}{27}}\right)^{1/3}, \quad \text{or} \quad (29b)$$

$$m_{1,2} = 2\sqrt{\frac{\alpha_2}{3}}\cos\left(\frac{\phi}{3} \pm \frac{2\pi}{3}\right), \qquad \alpha_2 > \frac{3}{\sqrt[3]{4}}, \quad (29c)$$

where

$$\cos\phi = \sqrt{\frac{27}{4\alpha_2^3}}. \quad (29d)$$

For $\alpha_2 = 3/\sqrt[3]{4}$ then $m_{1,2} = -1/\sqrt[3]{2}$, which is the degenerate case. The $\alpha_2 < 3/\sqrt[3]{4}$ case is of most interest and has a solution in the form

$$v = D_1 e^{-\lambda(x-x_s)}\cos\omega(x-x_s) + D_2 e^{-\lambda(x-x_s)}\sin\omega(x-x_s), \quad (30)$$

where $\lambda = (1/2)(A+B)$, $\omega = (\sqrt{3}/2)(A-B)$, and $x_s = l_t/l_m$. The remaining constants can be evaluated using the conditions (24c)–(24f). From the continuity conditions at $x = x_s$, we can show that

$$D_1 = C_1 v_1(x_s) + C_2 v_2(x_s), \quad (31a)$$

$$D_2 = \frac{1}{\omega}\{C_1[v_1'(x_s) + \lambda v_1(x_s)] + C_2[v_2'(x_s) + \lambda v_2(x_s)]\}, \quad (31b)$$

$$C_2 = -\frac{v_1'(x_s) + 2\lambda v_1'(x_s) + (\omega^2+\lambda^2)v_1(x_s)}{v_1'(x_s) + 2\lambda v_2'(x_s) + (\omega^2+\lambda^2)v_2(x_s)}C_1 = -KC_1. \quad (31c)$$

From (24f) we find:

$$C_1 = \left\{S_1 - KS_2 + \frac{1}{(\omega^2+\lambda^2)} \times [2\lambda v_1(x_s) - 2K\lambda v_2(x_s) + v_1'(x_s) - Kv_2'(x_s)]\right\}^{-1}, \quad (31d)$$

where

$$S_1 = \sum_{n=0}^{\infty}\frac{a_n}{n+2}x_s^{n+1}, \quad (32a)$$

$$S_2 = \sum_{n=0}^{\infty}\frac{b_n}{n+2}x_s^{n+1}. \quad (32b)$$

So, using back substitution, all the arbitrary constants can be evaluated and the solution is

$$v(x) = \begin{cases} C_1 v_1(x) + C_2 v_2(x), & x < x_s \\ e^{-\lambda(x-x_s)}[D_1\cos\omega(x-x_s) + D_2\sin\omega(x-x_s)], & x > x_s. \end{cases} \quad (33)$$

5. Results

We have examined the solution of the y-independent vorticity equation, with the slope-induced torque, for different ranges of l_t, l_m, and l_s. We have found that only when $l_t > l_m$, l_s (specifically $\alpha_1 > 1$ or equivalently $\sqrt{l_t l_s} > l_m$) the results are substantially different from the solution of the flat-bottom vorticity equation, which has already been investigated exhaustively and reported elsewhere (e.g., Pedlosky 1979, 1996). Furthermore, using a horizontal eddy viscosity of 100 m^2 s^{-1} (Bower et al. 1985), a bottom friction coefficient of 10^{-3} m s^{-1} (Csanady 1982), and typical length scales for the South Atlantic Bight, we get both l_s and l_m of order 10 km and l_t of about 100 km, which implies that the above condition is met.

Figure 3 shows the velocity and vorticity profiles when $l_m = l_s$. From the different l_t cases considered it may be appreciated that the axis of the boundary current is shifted offshore as the width of the slope increases, suggesting that the sloping topography has a significant influence on the dynamics of the western boundary current. Since the exact values of l_s and l_m are not known, it seems pointless to examine the model results with different values of these parameters.

Figure 4 shows the depth-integrated contribution of each term in the vorticity budget when $l_t = 2l_m = 2l_s$, whose solution is depicted in Fig. 3. Over most of the slope both the beta and bottom stress torque for constant water depth terms are negative and the equation is balanced due to the slope-induced bottom stress torque. Furthermore, the creation of positive vorticity by this torque results in an offshore shift of the current axis (Fig. 3).

6. Discussion

We have found that the vorticity equation derived from the vertically integrated momentum equations,

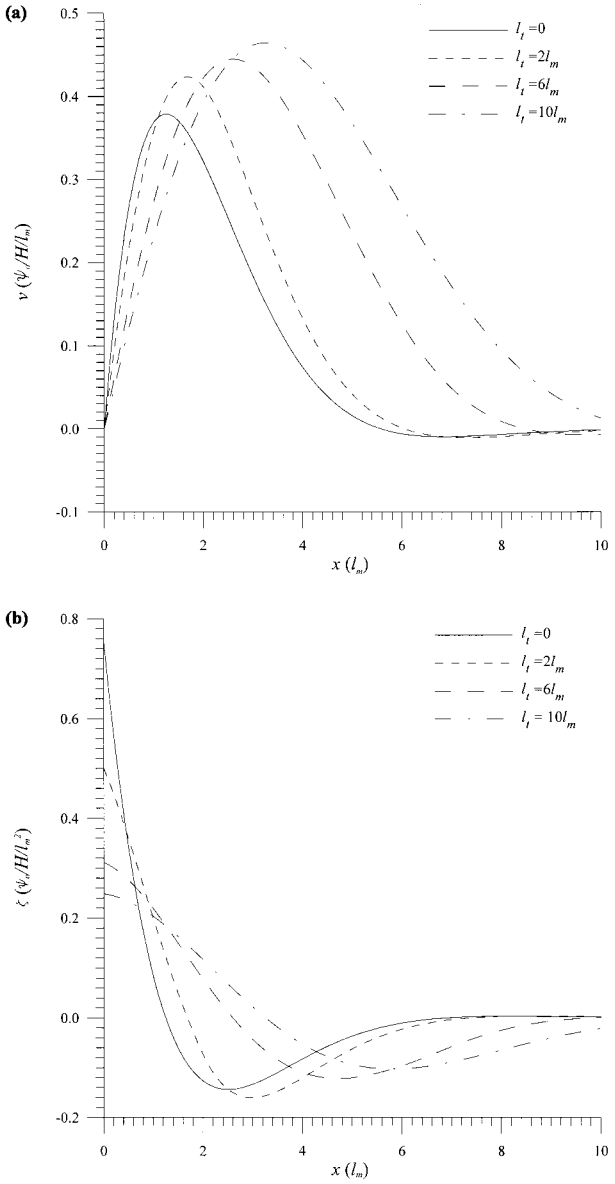

FIG. 3. Zonal structure of (a) velocity and (b) vorticity for l_t/l_m = 0, 2, 6, 10, and $l_s = l_m$ as inferred from Eq. (33).

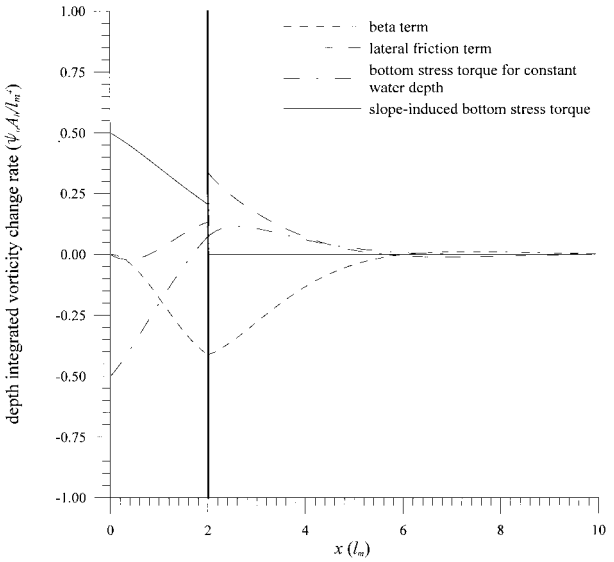

FIG. 4. Depth-integrated vorticity budget for $l_t = 2l_m$ and $l_s = l_m$ as inferred from Eq. (33).

with a linear bottom stress, introduces a new term that is interpreted as a slope contribution to the bottom stress torque. In his seminal study of the mean circulation in a coastal zone, Csanady (1978) had already incorporated a bottom stress torque that included the above contribution. In that paper Csanady obtained a vorticity equation similar to the vorticity equation for topographic wave generation, with linear friction replacing the time derivative, and its solution was named the arrested topographic wave. In that case the vorticity balance was between the torque by both surface and bottom stress and the torque by bottom pressure (see also Csanady 1982, p. 188). In the present study there is no external forcing and the steady-state solution corresponds to a balance between bottom stress torque and planetary vorticity advection. This could be thought of as a reverse Sverdrup balance, with poleward flow sustained by bottom stress torque.

a. Depth-averaged or geostrophic velocities

We have shown that in the case under consideration (depth-averaged flow is along isobaths) the bottom forcing in the depth-averaged and quasigeostrophic vorticity equations is exactly analogous, so our results may equally apply to one or the other. This fully analogous dependence makes us anticipate that the difference between the actual depth-averaged and geostrophic velocity and vorticity values will be small, but it seems worthwhile to briefly examine the size of this difference.

In our case the coastal constraint holds away from the coast, so $u_E\delta_E = -hu_g$, and using equation (9a) we get that the relation between the alongshore and cross-shore geostrophic velocities is given by $u_g = (rv_g)/(fh)$. The alongshore Ekman transport is then calculated as

$$v_E\delta_E = (ru_g/f) = r^2/(fh)^2 v_g h.$$

Hence, the cross-isobath geostrophic velocity (and transport) is a factor $r/(fh)$ smaller than the along-isobath geostrophic values, while the along-isobath Ekman transport is a factor $r^2/(fh)^2$ smaller than the along-isobath geostrophic transport. Similarly, by substituting the definition of the depth-averaged velocities [Eq. (8)] into $\zeta = \partial v/\partial x - \partial u/\partial y$ it may be shown that the difference between the depth-averaged and geostrophic vorticities will be of $(r/f)^2 d(v_g/h^2)/dx$, which is typically a factor $r^2/(fh)^2$ smaller than the geostrophic vorticity unless the slope dh/dx is very large.

If the dimensional bottom friction coefficient is given

by $r = 5 \times 10^{-4}$ m s^{-1}, for typical midslope depths of about 500 m, the $r/(fh)$ factor is about 0.01. This indicates that the cross-isobath geostrophic transport is much smaller than the alongshore geostrophic transport and clearly confirms that the alongshore Ekman transport is negligible. Equally, the difference between the depth-averaged and the geostrophic vorticity will be negligible.

When the depth-averaged flow is not along isobaths, then the bottom forcing will differ by as much as the cross-isobath term in Eq. (2) or (5). Because of the coastal constraint, however, this term will usually be small over the continental slope when the coast is sufficiently long. Far from the coast, for example, over seamounts, the cross-isobath term may be relatively important, and the solution of the depth-averaged and quasigeostrophic vorticity equations may substantially differ.

b. Potential vorticity conservation

In section 2 we examined the interior problem, forced through bottom Ekman pumping, for the particular case when the depth-averaged flow is along isobaths. In this case the Ekman bottom transport is compensated through geostrophic cross-isobath flow, which is exactly analogous to the slope-induced torque. It is illustrative to appreciate the role of the geostrophic cross-isobath flow by considering conservation of potential vorticity for the linear balance:

$$\frac{D}{Dt}\left(\frac{f}{h}\right) \equiv \frac{1}{h}\frac{Df}{Dt} - \frac{f}{h^2}\frac{Dh}{Dt} = 0, \tag{34}$$

where h here is the thickness of interior material columns. For the particular case of our analytical solution, that is, there are no changes in the y direction, this last equation becomes

$$\beta v_g = \frac{f}{h}u_g\frac{dh}{dx} + \frac{f}{h}\frac{\partial h}{\partial t}. \tag{35}$$

In general, the thickness of the interior column is modified through bottom Ekman pumping as

$$\frac{\partial h}{\partial t} = \frac{\partial(u_E\delta_E)}{\partial x} + \frac{\partial(v_E\delta_E)}{\partial y}. \tag{36}$$

In our case the second term in the right-hand side is zero because of the assumed y independence. Substituting back into Eq. (35) and using the expressions for bottom Ekman transport [Eq. (9)] we get

$$\beta v_g = \frac{f}{h}u_g\frac{dh}{dx} - \frac{r}{h}\frac{dv_g}{dx}. \tag{37}$$

Since there are no changes in the y direction, the depth-averaged continuity equation is

$$\frac{d(u_E\delta_E + u_g h)}{dx} = 0. \tag{38}$$

So, because of the coastal constraint, we get $u_E\delta_E = -u_g h$. Using Eq. (9a), we arrive at $u_g = (rv_g)/(fh)$. Substitution of this equation into Eq. (37) leads to our controlling equation (but without lateral friction):

$$\beta v_g = \frac{rv_g}{h^2}\frac{dh}{dx} - \frac{r}{h}\frac{dv_g}{dx} = -r\frac{d(v_g/h)}{dx}. \tag{39}$$

The first term on the right-hand side, proportional to dh/dx, is always positive (negative) for northward (southward) flow. The interpretation is that the stretching necessary for meridional flow takes place mainly through cross-isobath water movement.

At this point it is worthwhile to emphasize the potentially critical role played by the dynamics of the bottom boundary layer. In our very simple representation these dynamics are all hidden in the bottom friction coefficient, which we have chosen as constant. We have shown, however, that the bottom friction coefficient is indeed proportional to the vertical eddy viscosity, so this coefficient will surely change in the cross-isobath direction depending on the dynamics of the interior flow, inducing some type of feedback process. For the y independent case, the slope-induced bottom torque would need to be replaced by $v(rh^{-1})_x$.

c. Meridional integrated transport

An argument against the potential importance of Stommel's (1948) bottom friction model has been that where a western boundary current touches bottom, so that bottom friction is high, its curl integrates to zero because the velocity must be small at both sides of the stream (Csanady 1988). For a flat bottom the simplified balance between bottom stress curl and planetary vorticity advection is given by (again with dimensional variables)

$$\beta v = -\frac{r}{h}\frac{dv}{dx}, \tag{40}$$

and the poleward transport integrated across the western boundary section is zero:

$$\int_0^L vh\,dx = -\frac{r}{\beta}\int_0^L \frac{dv}{dx}\,dx = -\frac{r}{\beta}\int_{v(0)}^{v(L)} dv = 0. \tag{41}$$

This is not necessarily true anymore over the continental slope. In this case the simplified balance is

$$\beta v = -r\frac{d(v/h)}{dx}, \tag{42}$$

which, when integrated across the western boundary section, leads to

$$\int_0^L vh\,dx = \frac{r}{\beta}\left\{-\int_0^L \frac{dv}{dx}\,dx + \int_0^L \frac{v}{h}\frac{dh}{dx}\,dx\right\} = \frac{r\alpha}{\beta}\int_0^L \frac{v}{h}\,dx \tag{43}$$

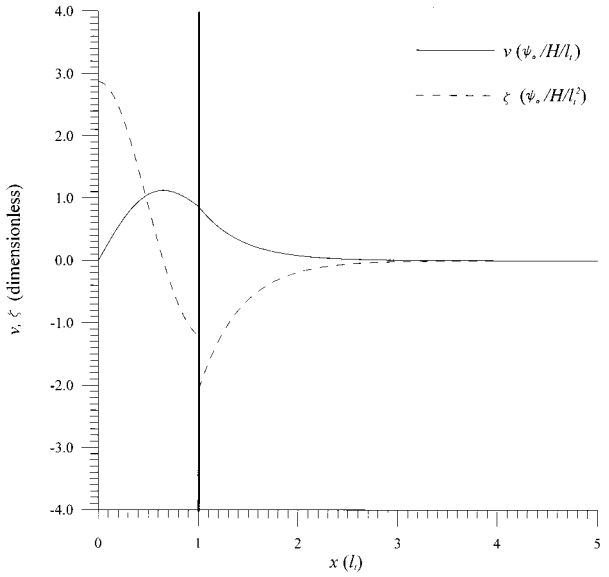

FIG. 5. Zonal structure of velocity and vorticity when $l_t = 2.4l_s$ as inferred from Eq. (45).

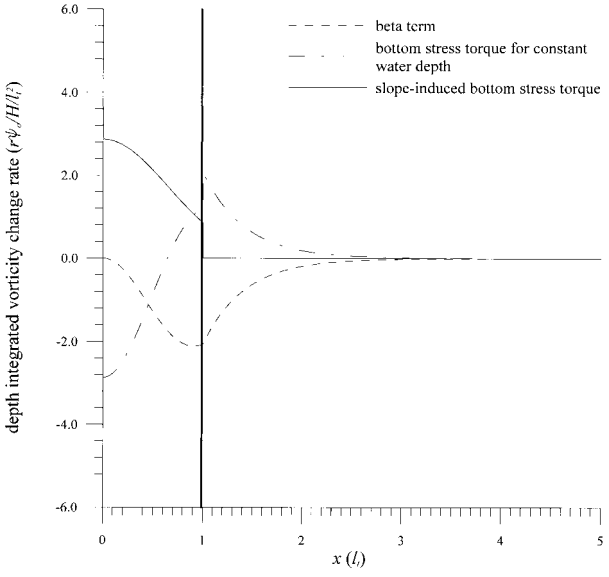

FIG. 6. Depth-integrated vorticity budget for $l_t = 2.4l_s$ as inferred from Eq. (45).

after using $dh/dx = H/l_t \equiv \alpha$. The total transport now depends on the ratio v/h, everywhere positive for northward flow.

d. The general solution to Eq. (42)

The general solution to Eq. (42) is

$$v = Ch \exp\left[-\frac{\beta}{r}\int_0^x h\, dx\right], \tag{44}$$

where C is the arbitrary constant. It is important to note that, since the layer depth $h(x)$ vanishes at the coast ($x = 0$), the no-slip condition is automatically satisfied. For the discontinuous shelf, the pressure must be continuous at the shelf break which, from the momentum equations, means that v must be continuous. The arbitrary constant C is related to the flow rate and can be readily determined by the matching condition.

The upshot is that the simple solution (44) of the quasigeostrophic vorticity equation (42), with only the bottom friction (including the slope-induced bottom friction) and beta terms, satisfies the no-slip condition even without lateral friction. Of course, this does not mean that the solution will be as realistic as the one that includes lateral friction. For a linear continental slope this solution becomes

$$v(x) = \begin{cases} \dfrac{v_o}{l_t}\exp\left(-\dfrac{\beta H l_t}{2r}\right)x \exp\left(-\dfrac{\beta H}{2rl_t}x^2\right) & \text{for } x < l_t \\ v_o \exp\left(-\dfrac{\beta H}{r}x\right) & \text{for } x > l_t, \end{cases} \tag{45}$$

which is illustrated in Fig. 5. It is to be noted that the vorticity is discontinuous at the shelf break (the matching point) due to the absence of lateral friction. Nevertheless, the solution is remarkably realistic, while providing a simple interpretation on the dynamics of western boundary currents.

The above solution illustrates that, as long as $l_t > l_s$, the axis of the alongshore stream is located over the continental slope, a feature frequently observed in many western boundary currents including the Gulf Stream in the South Atlantic Bight. A length scale for the offshore displacement of the stream axis is given by $L = \sqrt{2r/\beta\cdot\alpha}$, where $\alpha \equiv H/l_t$ is the bottom slope. This scale is identical to the width of the arrested topographic wave (Csanady 1978) provided that β replaces fk, where k is the wavenumber of the alongshore periodic wind stress forcing. The length scale may also be written as $L = (2\, l_t l_s)^{1/2}$, which is consistent with the observed feature that the flow moves offshore with increasing l_t. If $l_t < l_s$, then the length scale becomes l_s itself, which is the natural spatial scale arising from Eq. (42).

The depth-integrated vorticity budget is plotted in Fig. 6. It confirms that the main balance is between planetary vorticity advection and the slope-induced bottom stress torque, while the torque acting on constant depth columns has the same sign as planetary vorticity advection over most of the slope and changes sign over deep waters. The explanation for this is simple, as follows. The velocity increases from the western boundary to the stream axis so that the vorticity induced by the bottom stress curl (or torque on constant-depth water columns) is negative on the cyclonic side of the stream and positive on the anticyclonic side. On the other hand, the slope-induced bottom stress torque is positive over a steep slope because of the increasing difficulty for

bottom stress to act over the seaward-deepening water columns, despite its velocity also increasing seaward, and turns to zero off the slope.

7. Conclusions

We have examined the character of the homogeneous western boundary current flowing over the continental slope. Our formulation combines three highly idealized models: the Stommel model (Stommel 1948), the Munk model (Munk 1950), and the arrested topographic wave (Csanady 1978). The model is based on very crude representations of the Reynolds fluxes at the bottom by a linear bottom friction law, so we do not seek much realism in the details of the solution. Even so, this study clearly shows that the steepness of the continental slope does play a very important role in determining the structure of the western boundary current.

In our simple representation, with a northward flowing current independent of latitude and with a constant bottom friction coefficient, the main vorticity balance over the slope occurs between planetary vorticity advection and the slope-induced bottom torque. It is indeed the slope-induced torque that allows a nonzero integrated northward transport. Furthermore, this new term satisfies the no-slip condition, even in the absence of lateral viscosity. The simple solution for the case of no lateral viscosity shows that the position of the stream axis depends on the steepness of the slope. When the width of the continental slope, l_t, is larger than the Stommel scale, l_s, the scale for the offshore displacement of the stream axis is $(2\ l_t l_s)^{1/2}$.

We have further shown that, if the depth-averaged flow is along isobaths, the bottom stress torque term has the same dependence in both the depth-averaged and the quasigeostrophic vorticity equations; that is, the slope-induced torque caused by the geostrophic flow is exactly equal to the stretching due to cross-isobath geostrophic flow. In this circumstance the governing equation may be interpreted either as the one controlling the depth-averaged flow, the new term corresponding to a slope-induced torque, or as the equation controlling the interior geostrophic velocity, the new term corresponding to the cross-isobath geostrophic flow. In our particular model of the western boundary current, with all variables independent of latitude, the geostrophic and depth-averaged vorticity and alongshore velocities turn out to be numerically almost identical.

One question we should ask ourselves is what are we really trying to model—the depth-averaged or the geostrophic velocities? The formulation for the forcing role of the continental slope proposed here is quite general, so the answer to this question will depend on the specific problem under consideration. If we were modeling the coastal ocean, then the answer would certainly be the depth-averaged velocities, but, since we deal with boundary flows over the continental slope, then we are likely more interested in the geostrophic velocities. From this point of view it is correct to say that the latitude-independent continental slope allows water columns to move poleward by flowing offshore and stretching out.

In order to describe properly the role of the continental slope on the dynamics of the barotropic western boundary currents there are still many issues to be clarified. In particular it is important to clearly identify the role of alongshore pressure gradients (or across-isobath flow) and the characteristics of the bottom boundary layer over the slope, that is, the character of the feedback mechanism between the bottom boundary layer and the interior flow over the slope. Other effects, such as the influence of stratification and the dynamic instability of the boundary current, are undoubtedly very critical in controlling the actual bottom stress torque over the slope.

Acknowledgments. We are indebted to Gabe Csanady for a number of useful comments. The ideas in this paper would not have been possible without the inspiration arising from his enthusiasm and devoted lifelong work in oceanography, and we are very happy to dedicate this work to him. We are also thankful to our reviewers for several comments, in particular to one reviewer for his useful discussion of the particular case when the slope-induced bottom torque becomes equal to water column stretching. This work has been partly supported by the Spanish government (Grant MAR96-1893).

REFERENCES

Bower, A. S., H. T. Rossby, and J. L. Lillibridge, 1985: The Gulf Stream—Barrier or blender? *J. Phys. Oceanogr.,* **15,** 24–32.

Chapman, D. C., and S. J. Lentz, 1997: Adjustment of stratified flow over a sloping bottom. *J. Phys. Oceanogr.,* **27,** 340–356.

Csanady, G. T., 1976: Mean circulation in shallow seas. *J. Geophys. Res.,* **81,** 5389–5399.

——, 1978: The arrested topographic wave. *J. Phys. Oceanogr.,* **8,** 47–62.

——, 1979: The pressure field along the western margin of the North Atlantic. *J. Geophys. Res.,* **84,** 4905–4915.

——, 1982: *Circulation in the Coastal Ocean*. Reidel, 279 pp.

——, 1988: Ocean currents over the continental slope. *Advances in Geophysics*, Vol. 30, Academic Press, 95–203.

——, and J. L. Pelegri, 1995: Vorticity balance of boundary currents. *J. Mar. Res.,* **53,** 171–187.

Garrett, C., 1990: The role of secondary circulation in boundary mixing. *J. Geophys. Res.,* **95,** 989–993.

——, P. Rhines, and P. MacCready, 1993: Boundary mixing and arrested Ekman layers: Rotating stratified flow near a sloping boundary. *Annu. Rev. Fluid Mech.,* **25,** 291–323.

Gill, A. E., 1982: *Atmosphere–Ocean Dynamics*. Academic Press, 662 pp.

Griffiths, R. W., and G. Veronis, 1997: A laboratory study of the effects of a sloping side boundary on wind-driven calculation in a homogeneous ocean model. *J. Mar. Res.,* **55,** 1103–1126.

——, and ——, 1998: Linear theory of the effect of a sloping boundary on circulation in a homogeneous laboratory model. *J. Mar. Res.,* **56,** 75–86.

Holland, W. R., 1973: Baroclinic and topographic influences on the transport in western boundary currents. *Geophys. Fluid Dyn.,* **4,** 187–210.

Huang, R. X., 1991: The three-dimensional structure of wind-driven gyres: Ventilation and subduction. *Rev. Geophys.* (Suppl.: Contributions in Oceanography, U.S. National Report 1987–1990), 590–609.

Huthnance, J. M., 1984: Slope currents and ''JEBAR.'' *J. Phys. Oceanogr.,* **14,** 795–810.

Lentz, S. J., and J. H. Trowbridge, 1991: The bottom boundary layer over the northern California shelf. *J. Phys. Oceanogr.,* **21,** 1186–1201.

MacCready, P., and P. B. Rhines, 1991: Buoyant inhibition of Ekman transport on a slope and its effect on stratified spin-up. *J. Fluid Mech.,* **223,** 631–661.

——, and ——, 1993: Slippery bottom boundary layers on a slope. *J. Phys. Oceanogr.,* **23,** 5–22.

Munk, W. H., 1950: On the wind-driven ocean circulation. *J. Meteor.,* **7,** 79–93.

Pedlosky, J., 1979: *Geophysical Fluid Dynamics*. Springer-Verlag, 624 pp.

——, 1996: *Ocean Circulation Theory*. Springer-Verlag, 453 pp.

Salmon, R., 1992: A two-layer Gulf Stream over a continental slope. *J. Mar. Res.,* **50,** 341–365.

Sarkisyan, A. S., and V. F. Ivanov, 1971: Joint effect of baroclinicity and bottom relief as an important factor in the dynamics of ocean currents (English translation). *Izv. Acad. Sci. USSR, Atmos. Oceanic Phys.,* **7,** 173–188.

Shaw, P. T., and G. T. Csanady, 1983: Self-advection of density perturbations on a sloping continental shelf. *J. Phys. Oceanogr.,* **13,** 769–782.

Simons, T. J., 1979: On the joint effect of baroclinicity and topography. *J. Phys. Oceanogr.,* **9,** 1283–1287.

Stommel, H., 1948: The westward intensification of wind-driven ocean currents. *Trans. Amer. Geophys. Union,* **29,** 202–206.

Thorpe, S. A., 1987: Current and temperature variability on the continental slope. *Philos. Trans. Roy. Soc. London,* **323A,** 471–517.

——, P. Hall, and M. White, 1990: The variability of mixing at the continental slope. *Philos. Trans. Roy. Soc. London,* **331A,** 183–194.

Trowbridge, J. H., and S. J. Lentz, 1991: Asymmetric behavior of an oceanic boundary layer above a sloping bottom. *J. Phys. Oceanogr.,* **21,** 1171–1185.

Warren, B., 1963: Topographic influences on the path of the Gulf Stream. *Tellus,* **15,** 167–183.

Weatherly, G. L., 1972: A study of the bottom boundary layer of the Florida Current. *J. Phys. Oceanogr.,* **2,** 54–72.

White, F. M., 1991: *Viscous Fluid Flow*. McGraw-Hill, 614 pp.